ACCURATE SMALL-SIGNAL MODELLING OF A DOUBLE BARRIER RESONANT TUNNELLING DIODE (DBRTD)

C. V. Sammut, N. J. Cronin*, R. D. Schnell** and H. Tews**

University of Malta, Msida, Malta, * University of Bath, Bath, United Kingdom, ** Siemens Corporate Research and Development, Munich, Germany.

Abstract

Reflection measurements between 45 MHz and 13 Ghz on a DBRTD have resulted in a simple equivalent circuit model capable of predicting small-signal microwave properties to within ±5% of measurement. The device capacitance-voltage characteristic obtained is the most extensive published to date and has been determined for the first time using experimental data over the whole of the test frequency range.

1 Introduction

A number of equivalent circuit models for the resonant tunnelling diode (RTD) have appeared in the literature [1 - 10]. Most of these are based on the tunnel diode model with additional components introduced to fit the experimental observations. In some cases [2,7,8] CAD software was used to extract the intrinsic device equivalent circuit from embedded measurements which included effects pertaining to the test fixture. Since this increases the number of degrees of freedom for the fit, it may lead to a number of different device equivalent circuit configurations which are all equally capable of generating a simulated frequency response close to experimental observation. The lumped circuit elements thus extracted are not always readily identifiable with device properties and may lead to attributing properties to the intrinsic device which essentially pertain to the embedding network.

To date, very little progress has been made in measurements of the device equivalent capacitance-voltage ($C(V)$) characteristics and the scant data published so far has been based on single or restricted (low) frequency impedance measurements, often at insufficient bias voltages.

This work attempts to show that a simple tunnel diode equivalent circuit adequately explains the small-signal behaviour of a DBRTD over the frequency range 45 MHz to 13 GHz. Using accurate de-embedding techniques, reflection measurements lead to device equivalent circuit parameter extraction, and in particular, $C(V)$ is determined over relatively the widest bias voltage range reported so far and, for the first time, using data over the entire test frequency range.

2 Device structure and packaging

The resonant tunnelling heterostructure used in this work was grown on an n^+ GaAs substrate by MOCVD at Siemens Research Laboratories and consisted of 41 Å $Al_{0.6}Ga_{0.4}As$ barriers and a 50 Å GaAs quantum well. Symmetrical undoped GaAs spacer layers 300 Å thick clad this region and are followed by 1000 Å GaAs layers Si-doped to $1\times10^{17}cm^{-3}$. The initial GaAs buffer layer was 1 μm thick and doped to $2\times10^{18}cm^{-3}$. A 2000 Å GaAs layer (Si: $6\times10^{18}cm^{-3}$) facilitates the formation of ohmic contacts to the epilayer side. Details of the layer-growth have been published elsewhere [11].

A Ge/Au/Cr/Au ohmic contact layer was evaporated on the epilayer face and individual devices defined by lift-off. The devices were mesa-isolated by wet chemical etching using the metallisation as mask [11]. The substrate was lapped down to about 200 μm and a Ge/Au back contact evaporated. Individual diodes were diced into $300\times300\mu m^2$ chips. The device used in this study had an active area of $20\times20\mu m^2$ and was mounted in an E10/A package (LEW Techniques, Taunton, U.K.). The top contact was completed by means of a 12.5 μm-diameter gold wire spanned across the package flange and bonded in the middle onto the device epilayer metallisation. The $I-V$ characteristic is shown in figure 1 and was obtained by placing the packaged device in the mount of figure 2 with bias supplied through an HP11612A bias network. The unstable characteristic (solid line) was obtained by terminating the RF input port of the bias tee with a short circuit. Terminating this port with a 50 Ω load resulted in the stable characteristic (dotted line). Had the magnitude of the negative differential conductance been significantly larger, suppression of spurious oscillations would have presented problems [12].

3 The embedding network

We designed a coaxial mount (figure 2)

OF2

CH3277-1/93/0000-1041$01.00 © 1993 IEEE

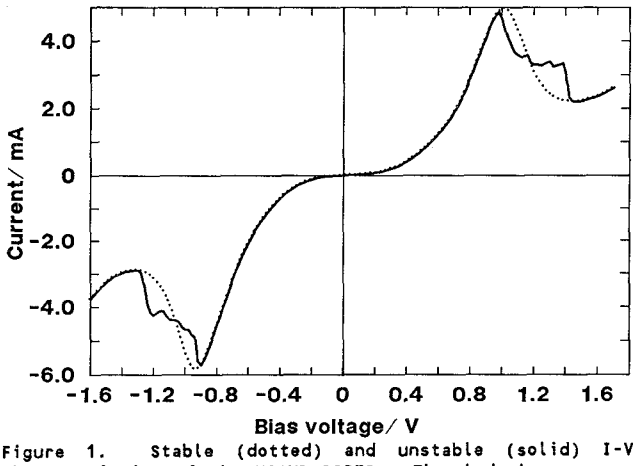

Figure 1. Stable (dotted) and unstable (solid) I-V characteristics of the MOCVD DBRTD. The dashed curve was obtained with the packaged device in the mount of figure 2 and biased through an HP11612A bias network, the rf input port of which was terminated by a 50 Ω load.

which mates directly with standard 3.5 mm or sma jacks and used the E10/A package in order to maintain a uniform coaxial system in our microwave measurements. The backshort is spring-loaded and presses the package against the centre conductor of the coaxial line.

Determination of device microwave properties necessitates transformation of S11 measurements to the device terminal plane in order to eliminate the intervening parasitics associated with the mount-package combination. The accuracy of the equivalent circuit representing this combination determines to a great extent the precision of the modelling parameters attributed to intrinsic device behaviour.

In determining the embedding network we have found it sufficient to assume the equivalent circuit shown in figure 2 to represent the package with the following physical significance attached to the circuit elements: L_1 = inductance of bond wire, L_2 = package inductance (assumed coaxial [13,14]), C_1 = capacitance between chip surface and top cap, C_2 = capacitance between pedestal and top cap.

S11 measurements between 45 MHz and 13 GHz were made on empty packages, a solid brass dummy package and open and short circuit packages using an HP8510B network

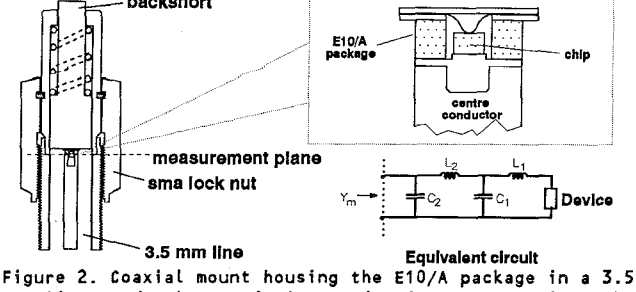

Figure 2. Coaxial mount housing the E10/A package in a 3.5 mm line and the equivalent circuit representing the package-mount parasitics; L_1 = 0.150 nH, L_2 = 0.252 nH, C_1 = 0.215 pF, C_2 = 0.0285 pF.

analyser fully calibrated at the package plane. The purpose of these measurements was to obtain trial estimates of the equivalent circuit parameters and subsequently refine these by curve-fitting first to the open circuit and then to the short circuit data.

The measured admittance with an empty package in the mount is approximately the susceptance of C_2. The dummy package is approximately equivalent to a coaxial inductance terminated by a backshort and thus allows an estimate of L_2 from the measured impedance.

The other packages were carefully constructed to emulate the actual packaged DBRTD. The open circuit package had a device chip of the same dimensions as the actual device soldered to the post. Since the bond wire in the real device perturbs the field in its vicinity, an identical wire was bonded across the package flange and the middle left close to but not touching the central device area. For this configuration, the circuit of figure 2 is reduced to L_2 flanked by C_1 and C_2 giving

$$1/(Y_m - j\omega C_2) - j\omega L_2 = 1/j\omega C_1 \qquad (1')$$

where Y_m is the admittance measured at the package plane. C_1 was estimated from the slope of (1') and parameter values subsequently adjusted to obtain the best fit of the calculated $Y_m(f)$ to the measured data.

The dummy chip mounted in the short circuit package was Au-coated on all six faces and was stitch-bonded as in the actual device. This configuration emulates the real situation more closely since the parasitic elements are nominally identical. The completed package had a dc resistance of less than 1 Ω. L_1 was estimated from the known length and diameter of the bond wire [15] and used along with the previous estimates as trial values in curve-fitting the parameters to the measured short circuit admittance shown in figure 3. The best fit was obtained with L_1 = 0.150 nH, L_2 = 0.252 nH, C_1 = 0.215 pF, C_2 = 0.0285 pF and a finite

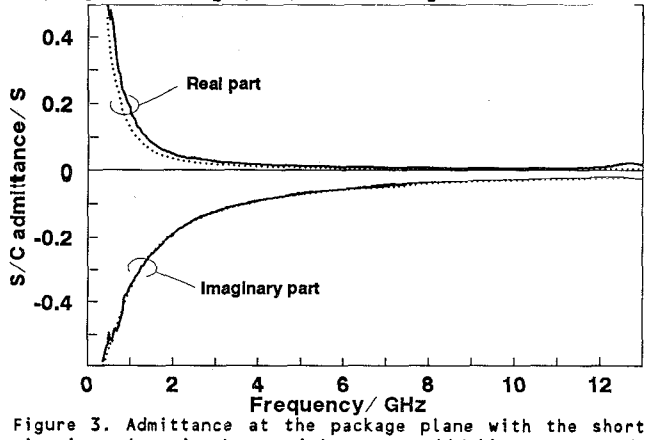

Figure 3. Admittance at the package plane with the short circuit package in the coaxial mount: solid line - measured, dotted line - calculated.

package resistance of 0.8 Ω in series with L_1. There is good agreement between the measured admittance and that simulated using these values; in particular, the susceptance plots are virtually coincident over the 45 MHz to 13 GHz test frequency range.

4 Device characterisation

S11 measurements were performed over the frequency range 45 MHz to 13 GHz at 86 different bias voltages between -1.5 and 1.7 V with an HP8510B network analyser in conjunction with an external voltage source which provided bias through the analyser bias port. The HP8510B was calibrated at the measurement plane and the test signal power was set to a nominal -20dBm.

The measurements were transformed through the package-mount equivalent circuit, determined as described in section 3, to obtain the device admittance, $Y_d(f)$ (figure 4). We have assumed a simple model for the DBRTD with differential resistance, $R(V)$ obtained from the dc $I-V$ characteristic, leaving the device capacitance, $C(V)$, to be determined from the reflection measurements. The model parameters were assumed to be frequency independent within the test frequency range. The series resistance, R_s, was determined as follows. Referring to figure 4, the device impedance, Z_d, is given by

$$\Re(Z_d) = R_s + \frac{R}{1+(\omega CR)^2} \quad (1)$$

$$\Im(Z_d) = -\frac{\omega CR^2}{1+(\omega CR)^2} \quad (2)$$

$C(V)$ may be estimated from **(2)** at any bias voltage using Z_d and the known $R(V)$. R_s is then found by substituting for C in **(1)**. A mean value of $R_s = 4.4 \pm 0.5\Omega$ was obtained over the test frequency range.

A more accurate method of determining $C(V)$ follows. The effect of R_s on Z_d is subtracted out to obtain an intrinsic admittance, Y_{intr};

$$Y_{intr}^{-1} = Z_d - R_s \quad (3)$$

$$i.e., \quad Y_{intr}(\omega) = G(V) + j\omega C(V)$$

where $G = 1/R$ is the differential conductance. The slope of the susceptance versus frequency plot then gives $C(V)$. The mean of $\Re\{Y_{intr}(\omega)\}$ over the frequency range gives another estimate of $G(V)$.

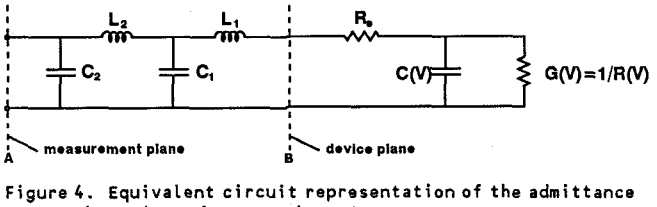

Figure 4. Equivalent circuit representation of the admittance measured at the reference plane A.

The percentage standard error in the slope of $\Im\{Y_{intr}(\omega)\}$ was found to be less than 3% with a negligible intercept at all bias voltages. The results are shown in figures 5 and 6.

Of particular interest are the $C(V)$ results since these are the most extensive published to date for a DBRT structure. The capacitance peaks in forward and reverse bias correspond to the respective peak voltages. This is due to charge accumulation in the quantum well at resonance. The secondary peaks in $C(V)$ at voltages near the extremities of the bias range may be due to a second, much more weakly-bound level in the quantum well. The $I-V$ characteristic (figure 1) does not show evidence for this, but at the corresponding voltages, the $G-V$ curve shows distinctive changes in dG/dV.

5 Simulation of experimental results

A convenient way of assessing the suitability and accuracy of the small-signal equivalent circuit model is to simulate the measured S11 as a function of frequency using the frequency-independent values of R_s, $C(V)$ and $G(V)$ determined as described above. The

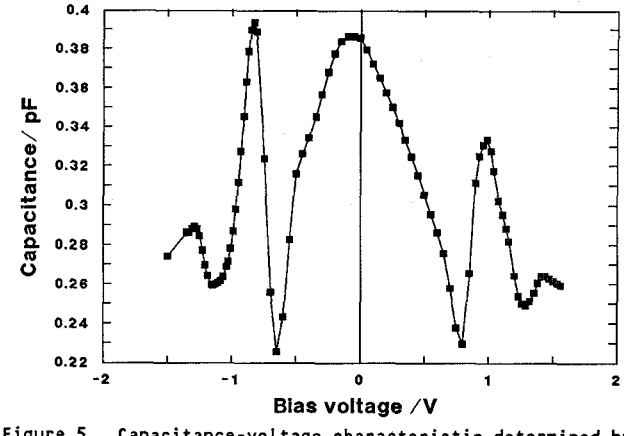

Figure 5. Capacitance-voltage characteristic determined by the analysis of reflection measurements as described in the text.

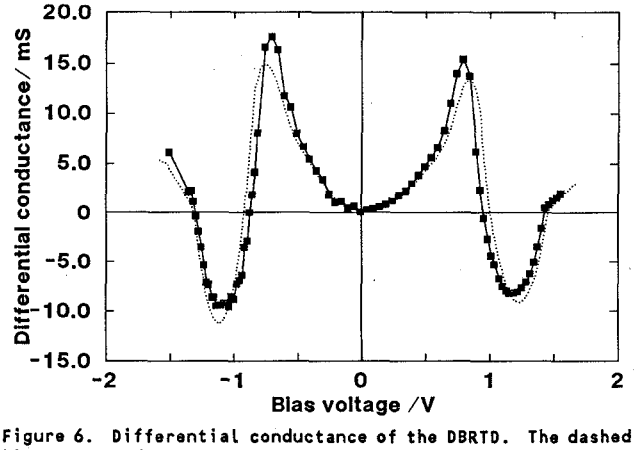

Figure 6. Differential conductance of the DBRTD. The dashed line was obtained by differentiating the I-V characteristic, while the points represent experimental values obtained as described in the text from the reflection measurements.

Smith chart plots shown in figure 7 where obtained by transforming the calculated device admittance through the package-mount equivalent circuit, thereby obtaining the reflection coefficient looking into plane A of figure 4. The maximum difference between experimental and simulated data was less than 5% over all bias voltages. This is the first small-signal study in which a resonant tunnelling device has been characterised at microwave frequencies at such a large number of bias voltages and the results fitted with high accuracy to the simple tunnel diode model.

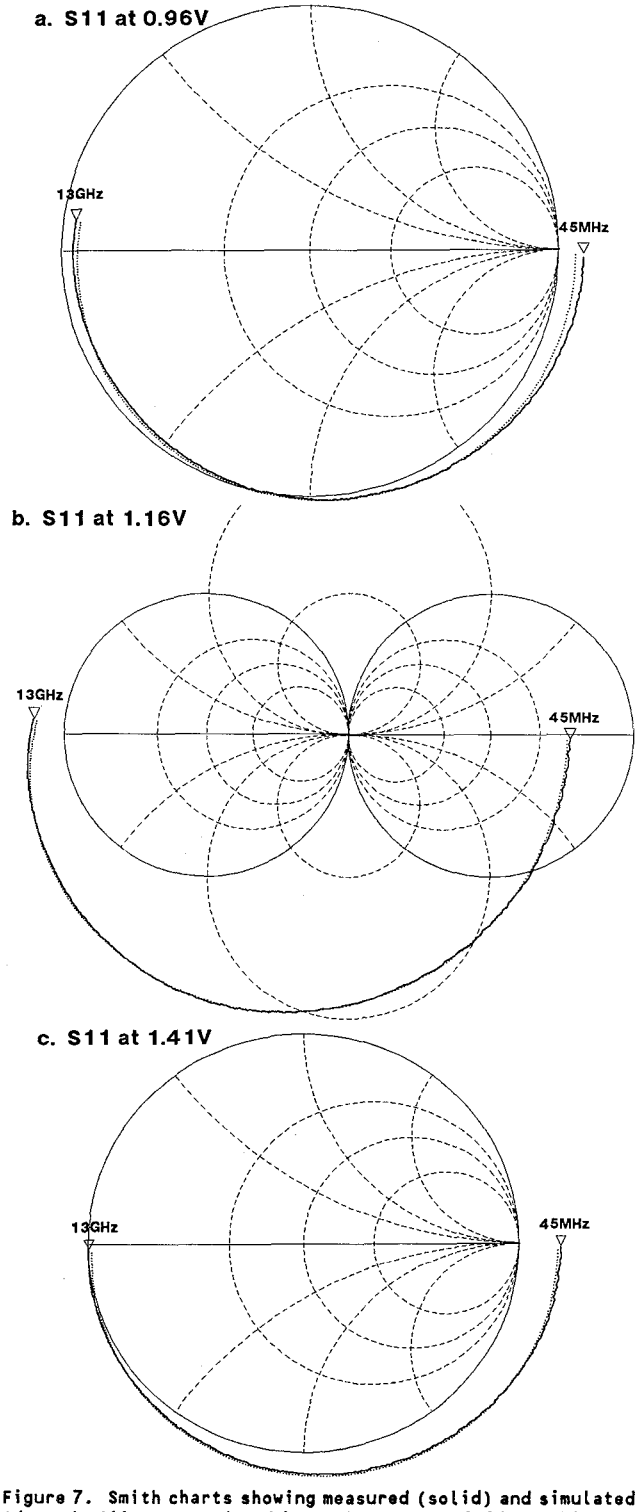

Figure 7. Smith charts showing measured (solid) and simulated (dotted) S11 at some key bias voltages; a) 0.96V, b) 1.16V, c) 1.41V.

6 Conclusion

We have determined a small-signal equivalent circuit model for a DBRTD over the frequency range 45 MHz to 13 GHz. This simple model is based on frequency-independent parameters and accurately predicts the small-signal properties of the device using voltage-dependent differential conductance, obtained from the dc $I-V$ characteristic, and capacitance determined over the entire test frequency range. We believe that this was made possible primarily by an accurate de-embedding technique which was facilitated by the choice of package and simple mount design which together allowed S11 measurements to be made within an almost entirely uniform 3.5 mm coaxial line.

The $C-V$ characteristic supplies important information on the physical processes involved in the operation of RTD's. We shall comment on this aspect elsewhere.

Finally, this model has been used with success in predicting the large-signal device behaviour in CAD analysis using the experimental results presented here [12].

References

1. T. J. Shewchuk, P. C. Chapin, J. M. Gering, P. D. Coleman, W. Kopp, and H. Morcoç, Proc. IEEE: Cornell Conf. Adv. Concepts High Speed Semicond. Dev. Circuits, Cornell University, New York, 1985, p 370.
2. J. M. Owens, D. J. Halchin, K. L. Lear, W. S. Lee, and J. S. Harris Jr., IEEE Int. Microwave Symp. Digest, 1989, p 471.
3. A. Zarea, A. Sellai, M. S. Raven, D. P. Steenson, J. M. Chamberlain, M. Henini, and O. H. Hughes, in W. Eccleston and P. J. Rosser, (ed.), ESSDERC 90, 20th European Solid State Dev. Res. Conf., Nottingham, IOP Publishing Ltd, 1990, p 559.
4. J. M. Gering, D. A. Crim, D. G. Morgan, and P. D. Coleman, J. Appl. Phys., Vol. 61, 1987, p 271.
5. J. M. Gering, T. J. Rudnick, and P. D. Coleman, IEEE Trans Microwave Theory Tech., Vol. MTT-36, 1988, p 1145.
6. A. Zarea, A. Sellai, M. S. Raven, D. P. Steenson, J. M. Chamberlain, M. Henini, and O. H. Hughes, Electron. Lett., Vol. 26, 1990, p 1522.
7. R. E. Miles, G. Millington, R. D. Pollard, D. P. Steenson, J. M. Chamberlain, and M. Henini, Electron. Lett., Vol. 27, 1991, p 427.
8. M. F. C. Schemmann, H. C. Heyker, J. J. M. Kwaspen, and Th. G. Van de Roer, IEE Proc.-H, Vol. 138, 1991, p 248.
9. D. Lippens and P. Mounaix, Electron. Lett., Vol. 24, 1988, p 1180.
10. P. Mounaix, P. Bedu, and D. Lippens, Electron. Lett., Vol. 27, 1991, p 1358.
11. R. D. Schnell, H. Tews, and R. Neumann, Electron. Lett., Vol. 25, 1989, p 830.
12. C. V. Sammut, "An investigation of the microwave properties of resonant tunnelling devices", PhD Thesis, University of Bath, U.K., 1992.
13. W. J. Getsinger, IEEE Trans. Microwave Theory Tech., Vol. MTT-14, 1966, p 58.
14. R. P. Owens, Electron. Lett., Vol. 7, 1971, p 580.
15. F. Longford-Smith, "Radio designers handbook", 4th ed., Iliffe, London, 1953.